

## RESEARCH ARTICLE

# Regionality of short and long period oscillators in the suprachiasmatic nucleus and their manner of synchronization

Tadamitsu Morimoto<sup>1</sup>, Tomoko Yoshikawa<sup>2</sup>, Mamoru Nagano<sup>1</sup>, Yasufumi Shigeyoshi<sup>1\*</sup>

**1** Department of Anatomy and Neurobiology, Graduate School of Medicine, Kindai University, Osaka-Sayama, Osaka, Japan, **2** Organization for International Education and Exchange, University of Toyama, Toyama, Japan

\*shigey@med.kindai.ac.jp

**OPEN ACCESS**

**Citation:** Morimoto T, Yoshikawa T, Nagano M, Shigeyoshi Y (2022) Regionality of short and long period oscillators in the suprachiasmatic nucleus and their manner of synchronization. PLoS ONE 17(10): e0276372. <https://doi.org/10.1371/journal.pone.0276372>

**Editor:** Shin Yamazaki, University of Texas Southwestern Medical Center, UNITED STATES

**Received:** June 6, 2022

**Accepted:** October 5, 2022

**Published:** October 18, 2022

**Peer Review History:** PLOS recognizes the benefits of transparency in the peer review process; therefore, we enable the publication of all of the content of peer review and author responses alongside final, published articles. The editorial history of this article is available here: <https://doi.org/10.1371/journal.pone.0276372>

**Copyright:** © 2022 Morimoto et al. This is an open access article distributed under the terms of the [Creative Commons Attribution License](https://creativecommons.org/licenses/by/4.0/), which permits unrestricted use, distribution, and reproduction in any medium, provided the original author and source are credited.

**Data Availability Statement:** Data used to generate the figures and supplementary figures in this manuscript are accessible on a public figshare repository (DOI: [10.6084/m9.figshare.21261324](https://doi.org/10.6084/m9.figshare.21261324)).

## Abstract

In mammals, the center of the circadian clock is located in the suprachiasmatic nucleus (SCN) of the hypothalamus. Many studies have suggested that there are multiple regions generating different circadian periods within the SCN, but the exact localization of the regions has not been elucidated. In this study, using a transgenic rat carrying a destabilized luciferase reporter gene driven by a regulatory element of *Per2* gene (*Per2::dLuc*), we investigated the regional variation of period lengths in horizontal slices of the SCN. We revealed a distinct caudal medial region (short period region, SPR) and a rostro-lateral region (long period region, LPR) that generate circadian rhythms with periods shorter than and longer than 24 hours, respectively. We also found that the core region of the SCN marked by dense VIP (vasoactive intestinal peptide) mRNA-expressing neurons covered a part of LPR, and that the shell region of the SCN contains both SPR and the rest of the LPR. Furthermore, we observed how synchronization is achieved between regions generating distinct circadian periods in the SCN. We found that the longer circadian rhythm of the rostral region appears to entrain the circadian rhythm in the caudal region. Our findings clarify the localization of regionality of circadian periods and the mechanism by which the integrated circadian rhythm is formed in the SCN.

## Introduction

The center of the mammalian circadian clock is located in the suprachiasmatic nucleus (SCN) of the hypothalamus, which consists of a bilateral pair of SCN across the third ventricle and contains approximately 10,000 cells on each side [1]. A mutual positive/negative feedback loop is formed by the regular expression of multiple clock genes: *Per1*, *Per2*, *Cry1*, *Cry2*, *Bmal1*, *Clock*, and their protein products [1, 2]. The clock gene expression rhythm within the SCN is robust, having a circadian rhythm of approximately 24 hours [2]. To maintain the integrated circadian rhythm as a single functional unit, the circadian rhythms in the oscillating neurons in the SCN must be synchronized.

Other data and further information are also available from the corresponding author on reasonable request.

**Funding:** The research was supported in part by JSPS KAKENHI (Grant-in-Aid for Scientific Research(C), Grant No; 19K06774 to T.Y., 20K07234 to N.M., 17K08580 to Y.S.). The funders had no role in study design, data collection and analysis, decision to publish, or preparation of the manuscript.

**Competing interests:** The authors have declared that no competing interests exist.

Functionally the SCN is divided into two regions [3]. The ventrolateral core region receives direct projection from the retina, while the dorsomedial shell region does not [3, 4]. The core region is composed of photo-responsive retinorecipient neurons that deliver photic information to the shell [3, 5]. After an abrupt shift of the light/dark cycle (LD cycle), the locomotor activity of rodents shows a slow shift in locomotor activity that is observed as jet lag [6]. We previously found a slow shift of the circadian rhythm in the shell after an abrupt shift of the LD cycle, and supposed that the slow shift causes jet lag [3].

The SCN is a heterogeneous structure comprising many types of neurons [1, 4, 7, 8]. Most SCN neurons are GABAergic, which is an inhibitory neurotransmitter [1, 4, 9]. Many of these GABAergic neurons co-express neuropeptides such as vasoactive intestinal peptide (VIP), gastrin releasing polypeptide (GRP), and arginine vasopressin (AVP) [1, 10]. AVP is expressed primarily in the shell of the SCN, while VIP and GRP are expressed in the core. VIP has been demonstrated to be particularly important for the maintenance and entrainment of cellular clocks in individual SCN neurons [11–14]. In addition, AVP-expressing neurons are densely expressed in the shell and have been shown to extend jet lag [15, 16]. Other neurotransmitters such as GABA and GRP may play additional roles for the maintenance of the circadian rhythm in the SCN [17–20].

Previous studies have suggested that each neuron in the SCN has a different cell-autonomous circadian rhythm [21, 22], and that there are regional period differences [21, 23–26]. Noguchi et al. [25, 26] dissected the SCN into dorsal-ventral and rostral-caudal coordination, and found differences in circadian period within the SCN. Koinuma et al. [21] revealed that there is a small region in the dorsomedial part of the ex-vivo coronal slices of the SCN, showing a shorter circadian period (short period region, SPR) than the rest of the SCN (long period region, LPR) and also revealed that a phase wave propagates from SPR to LPR. However, the localizations of these regions generating the various circadian rhythms within the SCN and how they are synchronized with each other has not been fully elucidated.

In this study, we investigated differences of circadian period in the rat SCN by monitoring the bioluminescence of coronal and horizontal slices. We observed and analyzed the regional period differences in the SCN, rostral-caudal coordination, and the relationship between the direction of the phase wave propagation and the period regionality. Furthermore, by dissecting the SCN slice into fragments, we investigated which region of the SCN determines the circadian period of the whole SCN and how the circadian rhythms are integrated within the SCN.

## Materials and methods

### Animals

Male transgenic rats of Wistar background carrying a bioluminescence reporter of *Period2* (*Per2*) expression were used. In these rats, the rat *Per2* promoter region was fused to a destabilized luciferase (*dLuc*) reporter gene [27]. The rats were bred and raised in our animal facility in Kindai University Faculty of Medicine under LD cycle with lights on/off at 7:00/19:00 or 19:00/7:00. Light intensity during the light phase was approximately 400 lux. Room temperature was 22 °C. The rats were fed commercial chow and tap water ad libitum. All the rats were two to three months old at the time of the experiments. All procedure was performed under isoflurane anesthesia, and all efforts were made to minimize suffering.

The experiments were conducted in accordance with the Kindai University Animal Experiment Regulations and the NIH Guidelines for the Care and Use of Laboratory Animals. All animal experimental procedures were approved by the Institutional Animal Experimentation Committee of Kindai University School of Medicine (Permission number: KAME-30-036).

## Slice preparation for ex-vivo cultures

Under deep anesthesia, an animal was decapitated between ZT0 and ZT12 (ZT, zeitgeber time), and the brain was harvested in ice-cold Hanks' balanced salt solution (pH 7.4, Sigma, USA). Coronal and horizontal brain slices were prepared by a Microslicer (Dosaka, Japan) at thicknesses of 200  $\mu\text{m}$  and 150  $\mu\text{m}$ , respectively. The region containing the SCN was dissected from the slices and placed on a culture insert (ORG50; Millipore, Germany) in 35-mm culture dishes with 1.3 mL of culture medium, DMEM (12100046, Gibco, USA) containing D-luciferin K salt (0.1 mM for PMT recording, 0.2 mM for imaging; DOJINDO, Japan) and supplemented with  $\text{NaHCO}_3$  (2.7 mM; Nacalai tesque, Japan), HEPES (10 mM; DOJINDO, Japan), kanamycin (20 mg/L; Gibco, Thermo Fisher Scientific, USA), insulin (5  $\mu\text{g}/\text{mL}$ ; Sigma, USA), putrescine (100 nM; Sigma, USA), apo-transferrin (100 mg/mL; Sigma, USA), progesterone (20 nM; Sigma, USA), and sodium selenite (30 nM; Gibco, USA) [28, 29].

## In situ hybridization

Digoxigenin-labeled r*Vip* (nucleotides 119–808; accession number X02341) cRNA probes were synthesized according to the manufacturer's protocol (Roche Diagnostics Japan, Japan). Horizontal brain slices (150  $\mu\text{m}$ ) were prepared as described above, fixed by immersing in 4% paraformaldehyde solution overnight, and processed using the free floating in situ hybridization method as described in our previous studies [6, 30]. In the present study, using this in situ hybridization technique, we detected the core region by the localization of *Vip* mRNA-containing neurons in horizontal SCN slices.

## Bioluminescence recording of coronal slices by PMT

Bioluminescence from cultured coronal slices of 200  $\mu\text{m}$  thickness was measured using a photomultiplier tube (PMT, Kronos; ATTO, Japan) for 1 in every 10 min at 37 °C. The measurements were started immediately after the slice preparation and continued for 7–14 days. The data between 12 and 132 hours in culture were used for analysis.

## Bioluminescence recording of horizontal slices by EMCCD camera

Horizontal slices of 150  $\mu\text{m}$  thickness were cultured under the same conditions except that the concentration of D-luciferin K salt was 0.2 mM. *Per2::dLuc* luminescence was recorded by one of three imaging systems: Multiversa, (ATTO, Tokyo, Japan) with an EMCCD camera (iXon 897, Andor, Belfast, UK; Exposure: 59 min., Em gain value: 500, Binning: 1 $\times$ 1) cooled at -90 °C; LUMINOVIEW (LV200, OLYMPUS, Japan) with an EMCCD camera (C9100-23B, Hamamatsu Photonics, Japan; Exposure: 29–59 min., Sensitivity gain: 150–200 (exposure 29 min.), 100–150 (exposure 59 min.), Gain: 1) cooled at -80 °C; or Cellgraph with an EMCCD camera (AB-3000, Atto, Japan; Exposure: 59 min., Electron Multiplier Gain: 300, Pre-Amplifier Gain: 1.0) cooled at -70 °C. Bioluminescence was recorded every 30 or 60 min. The measurement was started immediately after slice preparation and continued for 7 to 10 days. After the measurement, an integrated image of 24 to 120 hours was created using Image J, and the outline of the SCN was obtained from this image.

## Analysis of bioluminescence data to reveal the period and phase of the circadian rhythm

We set ROIs (ROI, regions of interest) dividing the SCN horizontal slices into several regions depending on the experiment. The average value of bioluminescence inside each ROIs was measured. The SCN horizontal slice was further divided into small square grids (grid size;

32  $\mu\text{m} \times 32 \mu\text{m}$ ). The raw data from PMT and cooled CCD camera were detrended by subtracting the 24-hour moving average [31, 32] and smoothed by taking a 5-point moving average [33]. The detrended and smoothed data from 24 hours to 120 hours after the beginning of recording were fitted to a mathematically generated damped cosine curve [21]  $\{y = a + b \cdot \exp(-c \cdot t) \cdot \cos 2\pi[(t + d) / e], t: \text{time}, a: \text{mesor}, b, c, d: \text{constants}, e: \text{period}\}$  using Excel Solver (Microsoft, USA). We calculated the period and phase of the circadian bioluminescence rhythm from each grid via the fitted curve. Grids with correlations  $< 0.6$  between detrended bioluminescence data and fitted curve were excluded from the analysis. Origin (OriginLab, USA) was used to visualize the circadian period from each grid.

### Statistical analysis

Repeated measures one-way ANOVA with post-hoc Bonferroni test was used to analyze the period length measured by PMT in coronal slices. To analyze the effect of forskolin (FK, adenylylate cyclase activator), we conducted repeated measures two-way ANOVA with post-hoc Bonferroni test, and multivariate comparison with post-hoc Tukey test. To analyze the effect of separation by a scalpel, we conducted repeated measures two-way ANOVA with post-hoc Bonferroni test.

## Results

### Phase mapping of circadian oscillations in horizontal slices of rat SCN

As shown in Fig 1A, horizontal SCN slices of 150  $\mu\text{m}$  thickness were prepared ( $n = 4$ ). In a slice, to examine how a phase-advanced or phase-delayed region relates to the core and the shell regions in the SCN, we investigated the localization of *Vip*-mRNA expressing neurons as a marker of the SCN core by using in situ hybridization [6] (Fig 1B). Then we examined the *Per2::dLuc* bioluminescence rhythm focusing on the difference along the rostro-caudal axis within the rat SCN, using a different individual from the one presented above. The phase wave of bioluminescence propagated from caudal to rostral and from medial to lateral in the SCN (Fig 1C, S1 Movie). The bioluminescence rhythm in the caudal area and in the medial area were the most advanced (Fig 1D and 1E, red) and those of the rostral and lateral areas were the most delayed (Fig 1D and 1E, blue). To examine this phase distribution within the SCN in more detail, we divided the SCN into small grids and analyzed them separately (Fig 1F). The phase was advanced in the medial-caudal area relative to the lateral-rostral area of the SCN. Comparing the phase map in the SCN horizontal slice (Fig 1F) with the localization of *Vip* mRNA expressing neurons (Fig 1B), *Vip*-expressing regions appeared to correspond to the regions with delayed phase within the SCN. In contrast, the shell included regions with both advanced and delayed phase.

### Circadian period analysis on consecutive coronal slices of SCN

We next investigated the difference in circadian period using consecutive coronal sections containing the SCN. Six consecutive 200  $\mu\text{m}$  coronal slices were prepared and were set into Kronos for examination of the *Per2::dLuc* circadian bioluminescence rhythm ( $n = 6$ ). Among them, clear circadian rhythms were detected from three or four SCN slices per animal. The circadian rhythm showing the largest amplitude was selected (Middle) along with the adjacent rostral (Rostral) and caudal sections (Caudal) (Fig 2A, S1 Fig). The mean values of the period length of the Rostral, Middle, and Caudal were  $23.8 \pm 0.2$ ,  $23.8 \pm 0.1$ , and  $22.4 \pm 0.2$  hours, respectively (Mean  $\pm$  SE, Fig 2B). The circadian period of Caudal was significantly shorter than those of the other two sections (Fig 2B), while no significant difference was detected

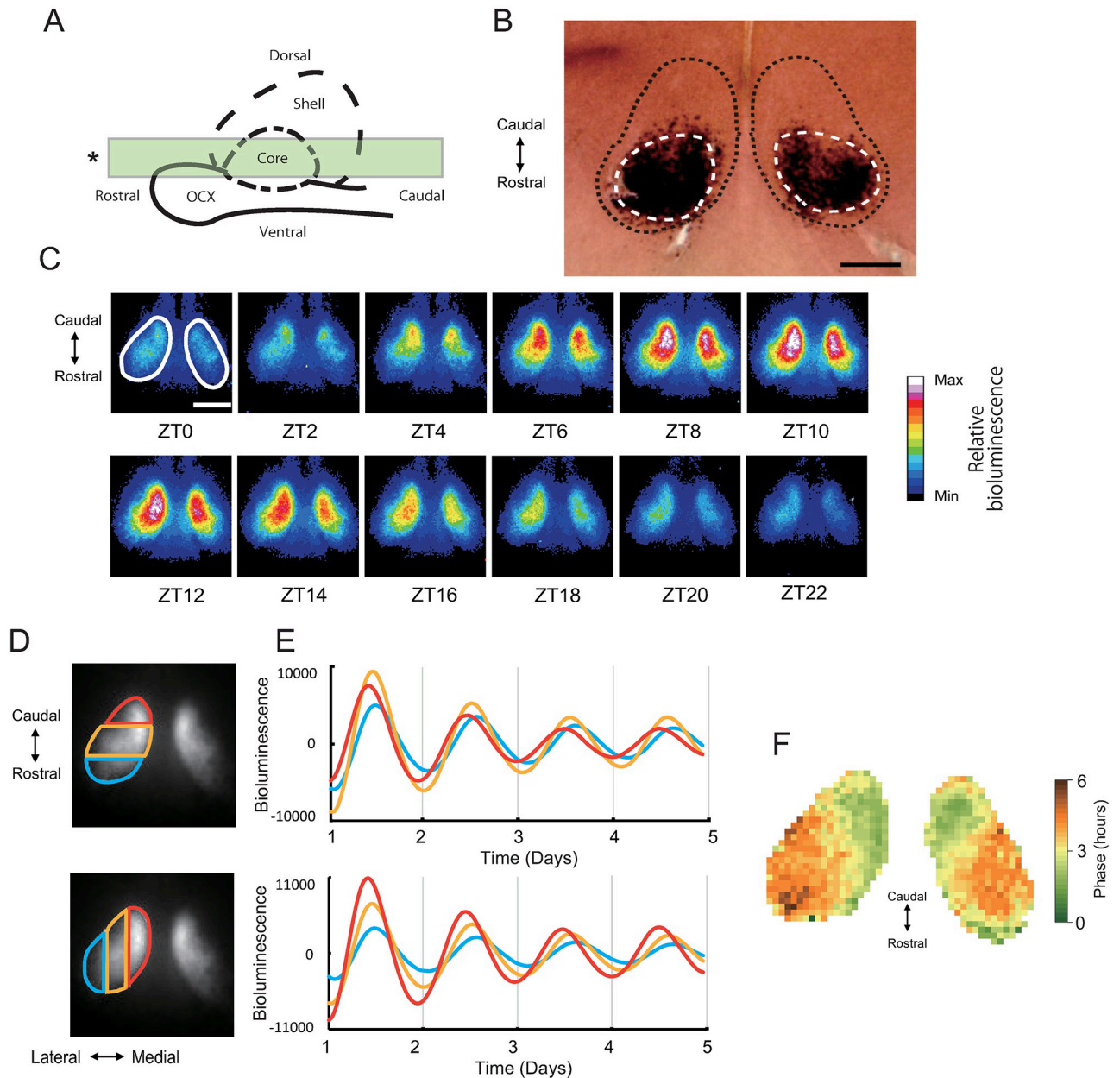


**Fig 1. Schema of the SCN slices and *Per2::dLuc* bioluminescence rhythm in the SCN.** (A) A schematic diagram of the sagittal section of the SCN (modified from Nagano et al., 2019). The outline of the SCN is denoted by a dashed line (considered as the shell region of the SCN), and the outline of the VIP region (considered as the core region of the SCN) by a dashed line. The green rectangle (\*) in the picture indicates the location of the horizontal slice excision for the present study. (B) Representative horizontal section of the SCN showing the *rVip*-expressing neurons by in situ hybridization. The outline of the core region was identified by *rVip*-expressing neurons. Black dashed line: outline of the SCN, White dashed line: core region of the SCN, Scale bar: 250  $\mu$ m. (C) Representative bioluminescence images of a horizontal slice of the rat SCN. White line indicates the outline of the SCN. The beginning of the first light period in the former light-dark cycle before decapitation was described as (projected) ZT0. Scale bar: 500  $\mu$ m. Data shown in C-F are from a single slice. (D) three ROIs were set on a unilateral SCN with the same rostro-caudal width and same medial-lateral width. (E) The average of the bioluminescence intensity of each ROI was plotted against time. The phase in the caudal ROI (red) are advanced compared to those of the middle (yellow) and rostral (blue) fragments (upper panel). The phases in the medial ROIs (red) are advanced compared to those of the middle (yellow) and lateral (blue) fragments (lower panel). (F) Phase map of 1<sup>st</sup> acrophase (after the first pZT0) of the SCN. This figure indicates that the phase wave propagates from the green region to the brown region. The phase was advanced in caudal and medial relative to the rostral and lateral, indicating that the phase wave propagates from the caudal side to the rostral side, and from the medial side to the lateral side. Grid size: 32  $\mu$ m.

<https://doi.org/10.1371/journal.pone.0276372.g001>

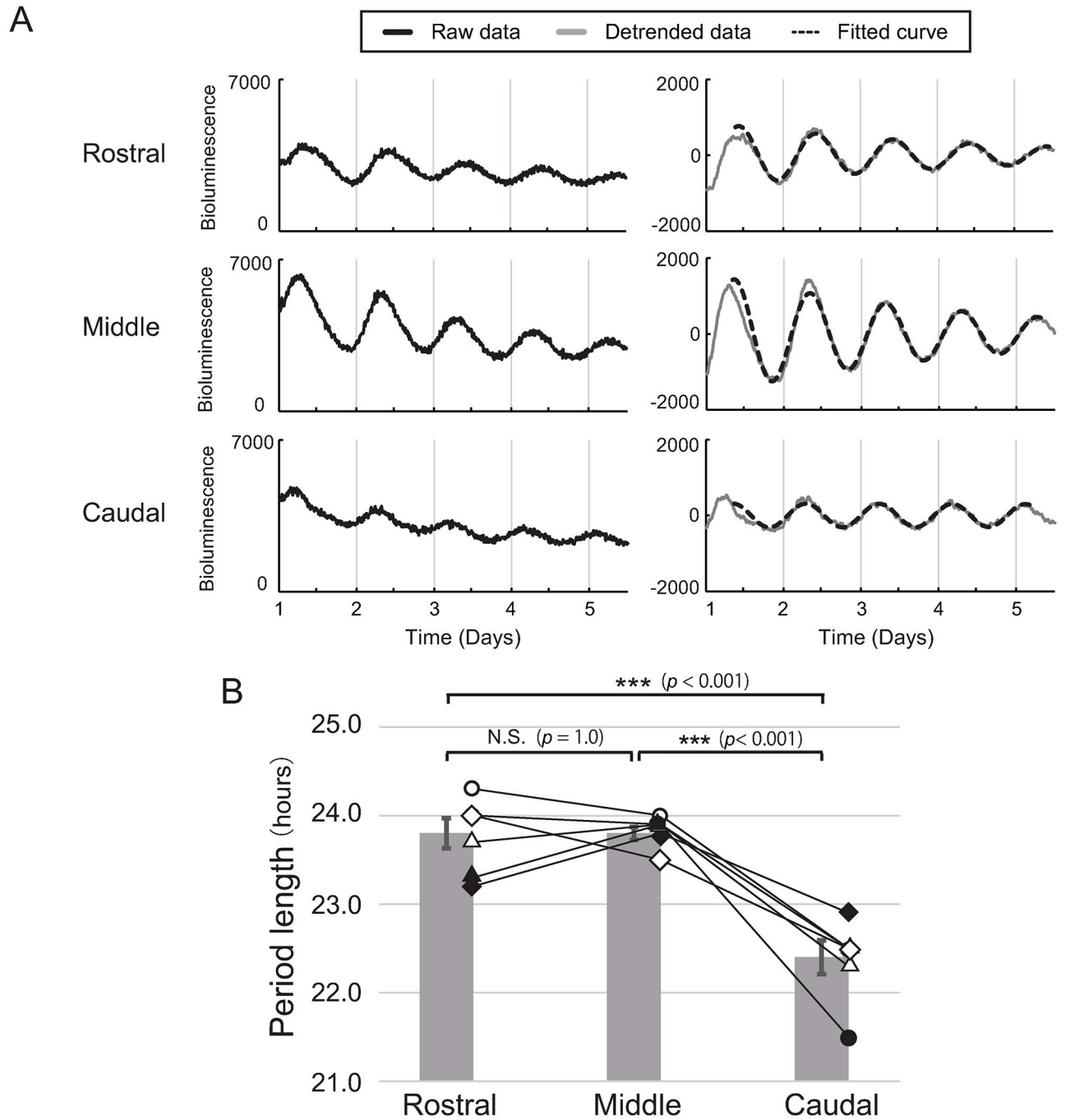


**Fig 2. *Per2::dLuc* bioluminescence rhythm in coronal slices of the SCN measured by PMT.** (A) Representative *Per2::dLuc* bioluminescence rhythm from consecutive slices of a single individual animal (Rostral, Middle, and Caudal). Left and right panels show raw data and detrended data, respectively. (B) Circadian periods from Rostral, Middle, and Caudal (Mean  $\pm$  SE). The periods of each slice are superimposed. Period data from the same individuals are connected by lines. Repeated measures one-way ANOVA with Post-hoc Bonferroni test. \*\*\*:  $p < 0.001$  vs Rostral and Middle, N.S.: not significant.

<https://doi.org/10.1371/journal.pone.0276372.g002>

between Rostral and Middle ( $p = 1.0$ ) (one-way ANOVA,  $F(2,4) = 23$ ,  $p = 0.0018$ ; post-hoc Bonferroni test, caudal vs rostral,  $p = 0.0055$ ; caudal vs middle,  $p = 0.0039$ ; rostral vs middle,  $p = 1.0$ ). These findings suggest that the caudal region of the SCN contains oscillators with shorter circadian periods than those in the middle and rostral regions.

### Effect of forskolin on circadian period in horizontal slice

To confirm the regional differences of circadian period, we disrupted the intracellular synchronization using *forskolin* (FK). Previously we found that FK disrupts the intercellular synchronization in the SCN [21, 34]. Horizontal slices of 150  $\mu\text{m}$  thickness were cultured in medium containing 10  $\mu\text{M}$  FK ( $n = 6$ ) or vehicle (DMSO). One to three horizontal slices were placed on a single culture insert, and bioluminescence was recorded by one of the EMCCD cameras. We set regions of interest (ROI) on the rostral half and caudal half of the unilateral SCN (Fig 3A), and designated them as Rostral area and Caudal area, respectively (Fig 3A). In FK treated horizontal slices, we found the circadian period of the Caudal area to be significantly shorter than that of the Rostral area (Fig 3B, S2 Movie). In contrast, the periods of the two areas were comparable in vehicle-treated cultures (Repeated measures two-way ANOVA, Rostral area vs Caudal area;  $F(1,10) = 8.2$ ,  $p = 0.017$ , Interaction;  $F(1,10) = 7.5$ ,  $p = 0.021$ . Post-hoc Bonferroni test; Rostral area vs Caudal area, Vehicle;  $p = 1.0$ , FK;  $p = 0.0016$ ). Further, we divided the SCN bioluminescence images into grids (64  $\times$  64  $\mu\text{m}$ ) for detailed analyses (Fig 3C). In the vehicle-treated cultures, the phase differences among the acrophases of the circadian rhythm in each grid were maintained from day 1 to day 5 (Fig 3C, upper panel). In contrast, in FK-treated cultures the phase difference among grids gradually increased (Fig 3C, lower panel). This difference is quantitatively shown in Fig 3D, which compares acrophase SD (standard deviation) within the SCN slices for each day in culture. The SDs of the 2<sup>nd</sup>–5<sup>th</sup> acrophases of the Caudal area were significantly larger than those of the Rostral area (Multivariate comparison, Caudal vs Rostral;  $F(1,117) = 14$ ,  $p = 0.0043$ , Peak 1<sup>st</sup>–5<sup>th</sup>;  $F(1,117) = 72$ ,  $p < 0.001$ , Interaction;  $F(4,117) = 8.7$ ,  $p < 0.001$ . Post-hoc Tukey test; Caudal vs Rostral; 1st,  $p = 0.1823$ ; 2nd,  $p < 0.001$ ; 3rd,  $p < 0.001$ ; 4th,  $p < 0.001$ ; 5th,  $p < 0.001$ , Vehicle vs FK; 1st,  $p = 0.9160$ ; 2nd,  $p = 0.0296$ ; 3rd,  $p < 0.001$ ; 4th,  $p < 0.001$ ; 5th,  $p < 0.001$ ). This finding suggested that FK administration caused desynchrony among circadian rhythms in the SCN. We divided the SCN into smaller grids (32  $\times$  32  $\mu\text{m}$ ) for further detailed analyses and visualized circadian period as a map. In FK-treated slices, we found the caudal region showed periods shorter than 24 hours (Fig 3E, S2B Fig). This region showing shorter periods (designated as short period region; SPR) occupied the caudal tip of the SCN and continued to the medial narrow area. In contrast, the circadian periods of other areas in the SCN were longer than 24 hours (designated as long period region; LPR).

### Effect of rostro-caudal separation on circadian period

Knowing the localization of SPR and LPR, we investigated which region is dominant when they are synchronized. Horizontal SCN slices with a thickness of 150  $\mu\text{m}$  was also divided into rostral and caudal fragments by scalpel ( $n = 7$ , Fig 4A). All fragments were placed on one culture insert and bioluminescence was recorded by EMCCD cameras. We set ROIs on the edges of the caudal, rostral and intact SCN, designating them Rostral, Caudal, and Intact, respectively, and the circadian periods of the bioluminescence from each ROI was measured. The circadian periods of Caudal were significantly shorter than those of Rostral (Fig 4B–4D) and Intact (Repeated measures one-way ANOVA, Rostral vs Caudal;  $F(2,12) = 12$ ,  $p = 0.0016$ , Post-hoc Bonferroni test; Intact vs Rostral,  $p = 1.0$ ; Intact vs Caudal,  $p = 0.0042$ ; Rostral vs Caudal,  $p = 0.0036$ ). Simultaneously, we prepared SCN slices without dividing by scalpel, and

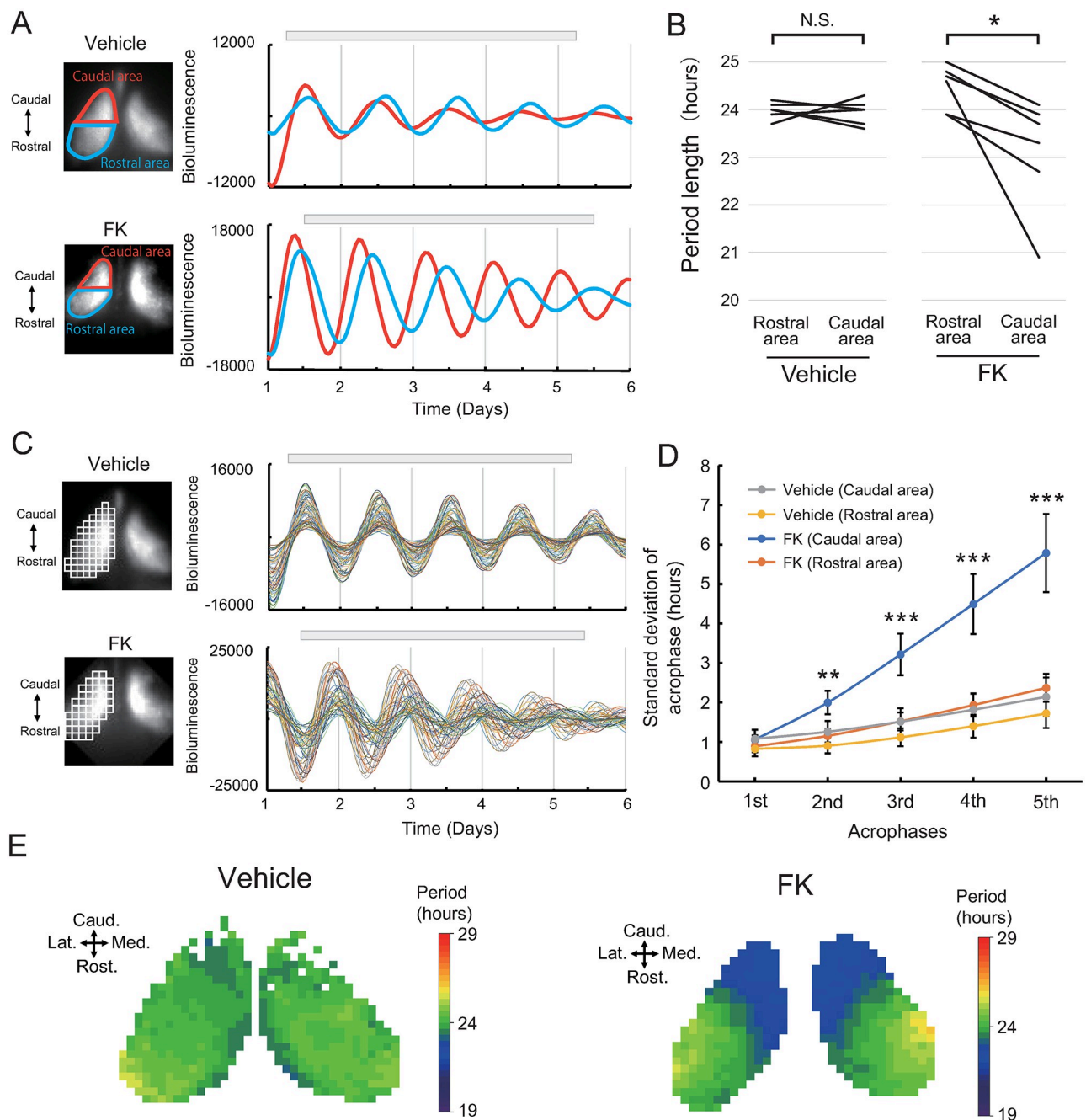


**Fig 3. Effect of forskolin on *Per2::dLuc* bioluminescence rhythm.** (A) Representative bioluminescence image of the SCN (left) and bioluminescence rhythm (right) of vehicle (upper panel) or FK-treated slices (lower panel). The average bioluminescence intensities of rostral (blue) and caudal (red) areas are plotted against time. Gray bars show the periods for curve fitting. The difference in period length between rostral and caudal areas increased in FK-treated slices. (B) Period lengths of the circadian rhythm in the rostral and caudal areas of the vehicle ( $n = 6$ ) and FK-treated ( $n = 6$ ) groups. The mean values of the bioluminescence periods of the rostral and caudal areas of the vehicle group were  $24.0 \pm 0.06$  hours,  $23.9 \pm 0.1$  hours, and in the FK-treated group,  $24.1 \pm 0.3$  hours and  $22.7 \pm 0.5$  hours, respectively (Mean  $\pm$  SE). Repeated measures two-way ANOVA with post hoc Bonferroni test showed no significant difference between rostral and caudal areas of Vehicle group, but showed a significant difference between rostral and caudal areas of FK-treated group (\*:  $p < 0.05$ , N.S.: not significant). (C) Small grids were used to divide the unilateral SCN, and bioluminescence data from all grids were plotted against time. With the vehicle, the period lengths were almost identical. In FK-treated slices, the circadian rhythms showed desynchrony compared with vehicle-treated slices. Gray bar: time used for curve fitting. Grid size:  $64 \mu\text{m}$ . (D) The standard deviation of acrophase in each (1<sup>st</sup>–5<sup>th</sup>) cycle within a single SCN slice (mean  $\pm$  SE). Acrophase was calculated by the fitted curve obtained from the bioluminescence of each grid. According to multivariate comparison and post-hoc Tukey test, there were significant differences between the rostral area and caudal area in phase variation of the 2<sup>nd</sup>–5<sup>th</sup> cycles (\*\*:  $p < 0.01$ , \*\*\*:  $p < 0.001$ ). (E) The period lengths of the circadian bioluminescence rhythms from grids were calculated by curve fitting. The period lengths of the vehicle-treated slice were similar, whereas the period lengths of the FK-treated slices showed shorter circadian rhythms in the caudal to medial grids than those in other grids. Med: medial, Lat: lateral. Grid size:  $32 \mu\text{m}$ .

<https://doi.org/10.1371/journal.pone.0276372.g003>



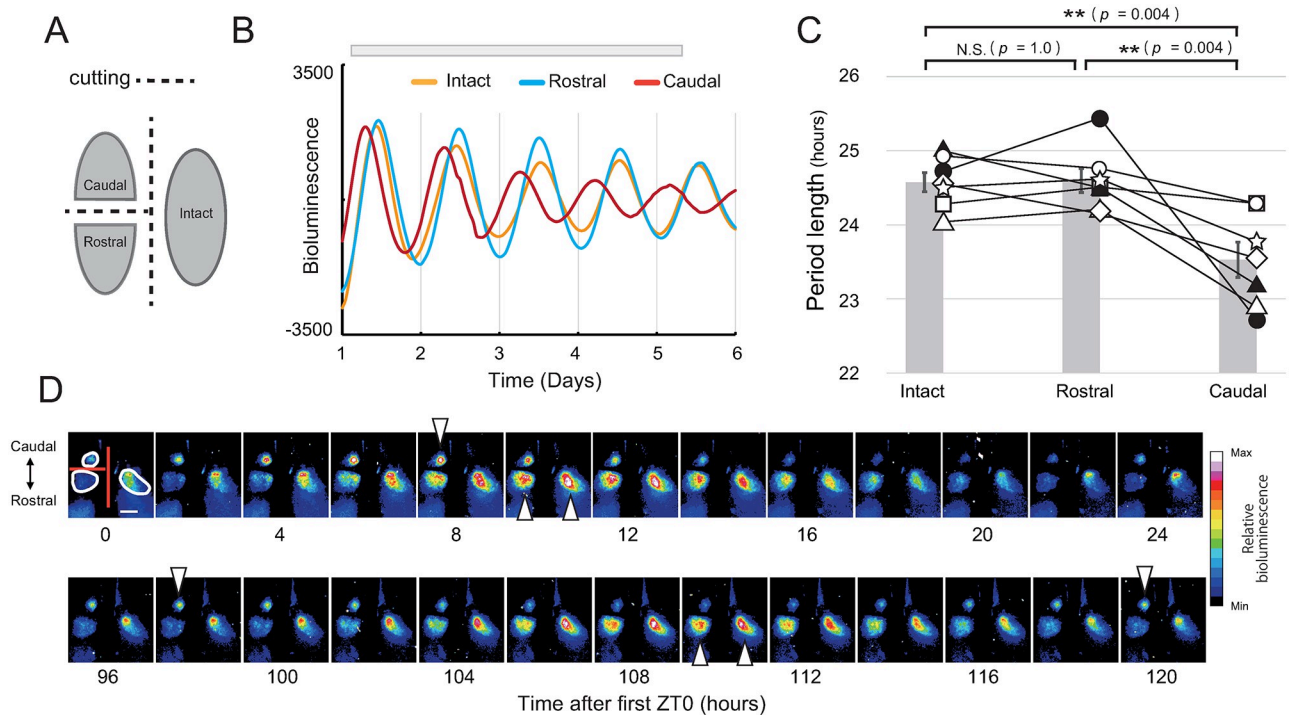


**Fig 4. Effect of rostro-caudal separation on *Per2::dLuc* bioluminescence rhythm.** (A) Schematic diagram of the dissected SCN. ROIs were set by outlines of Caudal, Rostral and Intact, and the circadian period of the bioluminescence from each ROI was measured. (B) One representative *Per2::dLuc* bioluminescence rhythm from three ROIs of a single slice. Gray bar indicates the period for curve fitting. (C) Circadian period of each ROI (n = 7). The period lengths were  $23.5 \pm 0.2$ ,  $24.6 \pm 0.2$ ,  $24.6 \pm 0.1$ , (Mean  $\pm$  SE) in Caudal, Rostral and Intact, respectively. Repeated measures one-way ANOVA with post-hoc Bonferroni test:  $**p < 0.01$ , N.S. = not significant. (D) Representative bioluminescence images of the SCN dissected by scalpel. White lines represent the outlines of Caudal, Rostral and Intact. White arrowheads indicate the peak phases of each fragment. Scale bar: 500  $\mu$ m.

<https://doi.org/10.1371/journal.pone.0276372.g004>

compared the circadian period with the intact side of the SCN dissected by scalpel (S3A Fig). We found that midline dissection of the SCN had no significant effect on the period length in horizontal SCN slices (S3B Fig).

## Discussion

In this study, by disrupting the synchrony among oscillating neurons, we found a region located mainly in the caudal area of the SCN showing circadian periods much shorter than 24 hours (SPR) in a horizontal slice culture of the SCN (Figs 2, 3 and S2 Fig). The direction of circadian phase wave propagation in the rat SCN detected by bioluminescence was from the SPR to other areas, which suggested that the SPR initiates the phase wave at the first step (Fig 1). Further, we dissected the SCN into rostral and caudal fragments by scalpel and found that the circadian period in the caudal fragment was much shorter than those in the rostral and intact SCN slices, which suggested that the circadian period of the rat SCN is determined by LPR rather than by SPR (Fig 4).

The localization of SPR in horizontal slices observed in the present study seems to be consistent with our previous study using coronal slice cultures [21]. In the previous study, we specified a narrow medial region of the SCN with a shorter *Per2* expression period (SPR) and found that the phase wave propagated from SPR to LPR [21]. In the present experiment, we also observed that the phase wave of *Per2* expression in SCN horizontal slices propagated from caudal to rostral and from medial to lateral (Fig 1C–1F), that is, from SPR to LPR. The narrow SPR at the middle of the SCN in the horizontal slice shown by FK treatment (Fig 3E) was

consistent with the morphological analysis of SPR in coronal sections in our previous study [21]. In addition, the direction of phase wave propagation was consistent between studies in that the wave started at the SPR and ended at the LPR. It is highly probable that the SPR observed in our previous study is identical to the SPR shown by the horizontal SCN slice analysis in the present study.

What mechanism binds the regions with distinct circadian periods? VIP and AVP are peptides that have been thoroughly investigated as substances synchronizing the oscillating neurons in the SCN [16, 35–37]. VIP is richly expressed among the neurons in the core of the SCN, and its receptor VPAC2 is mainly localized in the shell region of the SCN [15, 16]. VPAC2 gene deficient mice show desynchrony among oscillating neurons in the SCN [38]. In contrast, AVP-expressing neurons are mainly localized in the shell [25] and work to synchronize the oscillating neurons in the shell [26]. When dissected by scalpel, the caudal fragments contained the shell region and the rostral fragment contained both shell and core regions as shown in the *in situ* hybridization study showing the localization of VIP neurons as a core region marker (Fig 1B). AVP is abundantly expressed in the shell region of the SCN and contributes to maintaining the synchrony and phase difference among oscillating neurons in the SCN [15, 16]. Considering our present findings that there are regions with distinct intrinsic circadian periods within the SCN, synchronization of circadian oscillators by VIP and AVP contributes substantially to the circadian period of the SCN. On the other hand, Shinohara et al. [23] revealed that in rat suprachiasmatic nucleus slice cultures treated with antimetabolic drugs that decreased the number of glial cells, the release of arginine vasopressin and vasoactive intestinal polypeptide showed different circadian periods. The finding suggests that the glial cells are also involved in the synchrony of oscillating neurons in the SCN.

Differences in the circadian periods between VIP- and AVP-neurons might be involved in the regional differences in circadian period. Noguchi et al. [25, 26] reported that AVP cells have intrinsically short circadian periods and are entrained by VIP cells. These studies suggest that AVP- and VIP-expressing neurons have distinct circadian periods [23, 25, 26, 36]. In the present study, we divided the horizontal SCN slice into rostral and caudal fragments. As shown by the *in-situ* hybridization study (Fig 1B), most of the *Vip*-expressing neurons were contained in the rostral fragment. Therefore, it is possible that the shortening of the circadian period of the caudal fragment is due to the removal of the VIP-expressing neurons. However, this hypothesis that VIP neurons and AVP neurons respectively generate long and short circadian rhythms seems to be inconsistent with our present and previous findings [21] that the shell region contains both SPR and LPR. AVP are rich in the shell region, so the entire shell region would generate short circadian rhythms. However, this contradiction may be explained by the uneven localization of AVP-expressing neurons in the shell. AVP-expressing neurons are dense in the medial region and sparse in the lateral region of the shell [39, 40]. If AVP-neurons generate shorter circadian periods, it is possible that partial region of the shell containing dense AVP-neurons generates short circadian periods compared with those in other shell regions.

The SPR has similar characteristics to the morning oscillator (MO) in that it is localized in the caudal region and in that the phase wave propagation starts there. Many studies have suggested the existence of a distinct morning oscillator (MO) and evening oscillator (EO) within the SCN, as the activity rhythms of rodents are separated into two components under certain LD conditions [41–43]. Jagota et al. [44] measured electrophysiological activity in horizontal SCN slices of hamsters under varying LD cycles and found two distinct peaks, possibly representing the MO and EO. In more recent studies, a bioluminescence reporter has been used to investigate the localization of EO and MO in the SCN. Inagaki et al. [28] showed two groups of oscillators coupled to the onset and end of activity (indicating EO and MO) in the mouse

SCN. Another study by Yoshikawa et al. [45] mapped the localization of the two oscillators on the horizontal SCN slices in which the MO is located in the caudal tip of the SCN. In the present study, we found a region with a short circadian period in the caudal region of the SCN, and this region seemed to initiate the phase wave propagation. The finding is consistent with the properties of the MO reported previously [45]. Therefore, the present study suggested that SPR observed in the present study might be identical with the MO shown in other studies [43, 45].

In the present study, the vehicle group also showed differences in the circadian periods within the SCN (S2B Fig). The region that showed the short circadian period was mainly located in the caudal region where the SPR is, indicating that there was desynchrony even without FK. It is possible that the fragments of the SCN lost by preparing horizontal slices might be also necessary for the synchrony of oscillating neurons in the horizontal slices of the SCN. As shown in Fig 1A, the SCN slice culture did not contain the entire SCN. The lost fragment of SCN was essential for keeping the entire SCN synchronized. In addition, the retinohypothalamic tract, a neural projection from the retina to SCN, was also lost in this slice culture. It is possible that this loss also contributed to the desynchrony with vehicle treatment. Such structural disruptions and loss of components might be a limitation of slice culture experiments.

In conclusion, we analyzed the regional circadian period difference in the rat SCN and found that the phase wave propagates from the SPR to LPR. Further, we found that the circadian period of the caudal region is entrained by the rostral region of the SCN, which constitutes the overall integrated period of the whole SCN. The localization of the SPR and the direction of the phase wave propagation suggested that the SPR in the caudal region of the SCN may be identical to the MO of the two-oscillator model. The relationships between the SPR/LPR and MO/EO should be investigated further.

## Supporting information

**S1 Fig. *Per2::dLuc* bioluminescence rhythm by PMT from consecutive cultured coronal SCN slices.** A representative of the six specimens is shown in Fig 2A. Data from five other SCNs are shown. The gray lines and black dotted lines indicate the detrended wave forms and fitted curves, respectively.

(TIF)

**S2 Fig. Effect of FK on *Per2::dLuc* bioluminescence rhythm.** (A) Time series of bioluminescence images from SCN horizontal slices treated with vehicle (DMSO, upper panel) and forskolin (FK, lower panel). The numbers below the pictures indicate projected ZT (ZT, zeitgeber time). Scale bar: 500  $\mu$ m. (B) Grid analysis of circadian periods of *Per2::dLuc* bioluminescence rhythms. Grid size: 32  $\mu$ m.

(TIF)

**S3 Fig. Effect of separating right and left SCN in a horizontal slice.** (A) ROIs were set on the SCN with and without dissection. Mean bioluminescence rhythm from each ROIs were measured. The periods of bioluminescence rhythms from the SCN without dissection (left (a) and right (b), left picture, Dissection(-), n = 5) and from unilateral SCN with dissection along the midline but without rostro-caudal dissection ((c), right picture, Dissection(+), n = 7). Dashed lines in the right picture indicate the dissection lines. (B) Statistical analysis between Dissection(-) and Dissection(+) groups. Bioluminescence period was  $24.8 \pm 0.14$ ,  $24.9 \pm 0.16$  hours for Dissection(-) group (Mean  $\pm$  SE, Left and Right respectively), and  $24.6 \pm 0.13$  hours for Dissection(+) group (Intact). No significant difference was found by repeated measures one-way ANOVA with a post hoc Bonferroni test between right and left SCN without dissection (a

and b) and with dissection (c) (repeated measures one-way ANOVA;  $F(2,8) = 1.4$ ,  $p = 0.31$ : post-hoc Bonferroni test; a vs. b,  $p = 1.0$ , a vs. c,  $p = 1.0$ , b vs. c,  $p = 0.42$ ).

(TIF)

**S1 Movie. Bioluminescence imaging of a horizontal SCN slice without any treatment.** The number in the lower right corner indicates the elapsed time from the start of the measurement.

(AVI)

**S2 Movie. Bioluminescence imaging of a horizontal SCN slice with FK treatment.** The number in the lower right corner indicates the elapsed time from the start of the measurement.

(AVI)

## Acknowledgments

We thank Dr. Seiichi Hashimoto (Astellas Pharma Inc.) for the supply of *Per2-dLuc* transgenic rats. We also thank Ms. E. Uemukai and Ms. Y. Yoshikawa for the care and management of laboratory animals and laboratory materials.

## Author Contributions

**Conceptualization:** Tadimitsu Morimoto, Mamoru Nagano, Yasufumi Shigeyoshi.

**Data curation:** Tadimitsu Morimoto, Tomoko Yoshikawa, Mamoru Nagano.

**Formal analysis:** Tadimitsu Morimoto, Tomoko Yoshikawa, Yasufumi Shigeyoshi.

**Funding acquisition:** Tomoko Yoshikawa, Mamoru Nagano, Yasufumi Shigeyoshi.

**Supervision:** Yasufumi Shigeyoshi.

**Writing – original draft:** Tadimitsu Morimoto.

**Writing – review & editing:** Tadimitsu Morimoto, Tomoko Yoshikawa, Mamoru Nagano, Yasufumi Shigeyoshi.

## References

1. Welsh DK, Takahashi JS, Kay SA. Suprachiasmatic Nucleus: Cell Autonomy and Network Properties. *Annu Rev Physiol.* 2010; 72: 551–577. <https://doi.org/10.1146/annurev-physiol-021909-135919> PMID: 20148688
2. Reppert SM, Weaver DR. Coordination of circadian clocks in mammals. *Nature.* 2002; 418: 935–941. Available: <https://www.nature.com/articles/nature00965>
3. Nagano M, Adachi A, Nakahama K, Nakamura T, Tamada M, Meyer-Bernstein E, et al. An Abrupt Shift in the Day/Night Cycle Causes Desynchrony in the Mammalian Circadian Center. *J Neurosci.* 2003; 23: 6141–6151. <https://doi.org/10.1523/JNEUROSCI.23-14-06141.2003> PMID: 12853433
4. Herzog ED, Hermanstyn T, Smyllie NJ, Hastings MH. Regulating the suprachiasmatic nucleus (SCN) circadian clockwork: Interplay between cell- autonomous and circuit-level mechanisms. *Cold Spring Harb Perspect Biol.* 2017; 9. <https://doi.org/10.1101/cshperspect.a027706> PMID: 28049647
5. Shigeyoshi Y, Taguchi K, Yamamoto S, Takekida S, Yan L, Tei H, et al. Light-induced resetting of a mammalian circadian clock is associated with rapid induction of the mPer1 transcript. *Cell.* 1997; 91: 1043–1053. [https://doi.org/10.1016/s0092-8674\(00\)80494-8](https://doi.org/10.1016/s0092-8674(00)80494-8) PMID: 9428526
6. Nagano M, Ikegami K, Minami Y, Kanazawa Y, Koinuma S, Sujino M, et al. Slow shift of dead zone after an abrupt shift of the light-dark cycle. *Brain Res.* 2019; 1714: 73–80. <https://doi.org/10.1016/j.brainres.2019.02.014> PMID: 30771316

7. Silver R, Schwartz WJ. The suprachiasmatic nucleus is a functionally heterogeneous timekeeping organ. *Methods Enzymol.* 2005; 393: 451–465. [https://doi.org/10.1016/S0076-6879\(05\)93022-X](https://doi.org/10.1016/S0076-6879(05)93022-X) PMID: 15817305
8. Antle MC, LeSauter J, Silver R. Neurogenesis and ontogeny of specific cell phenotypes within the hamster suprachiasmatic nucleus. *Dev Brain Res.* 2005; 157: 8–18. <https://doi.org/10.1016/j.devbrainres.2005.02.017> PMID: 15939080
9. Ono D, Honma K-i, Honma S. GABAergic mechanisms in the suprachiasmatic nucleus that influence circadian rhythm. *J Neurochem.* 2021; 157: 31–41. <https://doi.org/10.1111/jnc.15012> PMID: 32198942
10. Patton AP, Hastings MH. The suprachiasmatic nucleus. *Curr Biol.* 2018; 28: R816–R822. <https://doi.org/10.1016/j.cub.2018.06.052> PMID: 30086310
11. Harmar AJ, Marston HM, Shen S, Spratt C, West KM, Sheward WJ, et al. The VPAC(2) receptor is essential for circadian function in the mouse suprachiasmatic nuclei. *Cell.* 2002; 109: 497–508. [https://doi.org/10.1016/S0092-8674\(02\)00736-5](https://doi.org/10.1016/S0092-8674(02)00736-5) PMID: 12086606
12. Aton SJ, Herzog ED. Come together, right . . . now: Synchronization of rhythms in a mammalian circadian clock. *Neuron.* 2005; 48: 531–534. <https://doi.org/10.1016/j.neuron.2005.11.001> PMID: 16301169
13. Maywood ES, Reddy AB, Wong GKY, O'Neill JS, O'Brien JA, McMahon DG, et al. Synchronization and maintenance of timekeeping in suprachiasmatic circadian clock cells by neuropeptidergic signaling. *Curr Biol.* 2006; 16: 599–605. <https://doi.org/10.1016/j.cub.2006.02.023> PMID: 16546085
14. Harmar AJ, Fahrenkrug J, Gozes I, Laburthe M, May V, Pisegna JR, et al. Pharmacology and functions of receptors for vasoactive intestinal peptide and pituitary adenylate cyclase-activating polypeptide: IUPHAR Review 1. *Br J Pharmacol.* 2012; 166: 4–17. <https://doi.org/10.1111/j.1476-5381.2012.01871.x> PMID: 22289055
15. Yamaguchi Y, Suzuki T, Mizoro Y, Kori H, Okada K, Chen Y, et al. Mice genetically deficient in vasopressin V1a and V1b receptors are resistant to jet lag. *Science (80-).* 2013; 342: 85–90. <https://doi.org/10.1126/science.1238599> PMID: 24092737
16. Kori H, Yamaguchi Y, Okamura H. Accelerating recovery from jet lag: prediction from a multi-oscillator model and its experimental confirmation in model animals. *Nat Publ Gr.* 2017; 1–10. <https://doi.org/10.1038/srep46702> PMID: 28443630
17. Da Li J, Burton KJ, Zhang C, Hu SB, Zhou QY. Vasopressin receptor V1a regulates circadian rhythms of locomotor activity and expression of clock-controlled genes in the suprachiasmatic nuclei. *Am J Physiol—Regul Integr Comp Physiol.* 2009; 296: 824–830. <https://doi.org/10.1152/ajpregu.90463.2008> PMID: 19052319
18. Liu C, Reppert SM. GABA synchronizes clock cells within the suprachiasmatic circadian clock. *Neuron.* 2000; 25: 123–128. [https://doi.org/10.1016/S0896-6273\(00\)80876-4](https://doi.org/10.1016/S0896-6273(00)80876-4) PMID: 10707977
19. Maywood ES, Chesham JE, O'Brien JA, Hastings MH. A diversity of paracrine signals sustains molecular circadian cycling in suprachiasmatic nucleus circuits. *Proc Natl Acad Sci U S A.* 2011; 108: 14306–14311. <https://doi.org/10.1073/pnas.1101767108> PMID: 21788520
20. Aida R, Moriya T, Araki M, Akiyama M, Wada K, Wada E, et al. Gastrin-Releasing Peptide Mediates Photic Entrainable Signals to Dorsal Subsets of Suprachiasmatic Nucleus via Induction of Period Gene in Mice. *Mol Pharmacol.* 2002; 61: 26 LP–34. <https://doi.org/10.1124/mol.61.1.26> PMID: 11752203
21. Koinuma S, Asakawa T, Nagano M, Furukawa K, Sujino M, Masumoto K-H, et al. Regional circadian period difference in the suprachiasmatic nucleus of the mammalian circadian center. *Eur J Neurosci.* 2013; 38: 2832–2841. <https://doi.org/10.1111/ejn.12308> PMID: 23869693
22. Welsh DK, Logothetis DE, Meister M, Reppert SM. Individual neurons dissociated from rat suprachiasmatic nucleus express independently phased circadian firing rhythms. *Neuron.* 1995; 14: 697–706. [https://doi.org/10.1016/0896-6273\(95\)90214-7](https://doi.org/10.1016/0896-6273(95)90214-7) PMID: 7718233
23. Shinohara K, Honma S, Katsuno Y, Abe H, Honma K. Circadian rhythms in the release of vasoactive intestinal polypeptide and arginine-vasopressin in organotypic slice culture of rat suprachiasmatic nucleus. *Neurosci Lett.* 1994; 170: 183–6. [https://doi.org/10.1016/0304-3940\(94\)90269-0](https://doi.org/10.1016/0304-3940(94)90269-0) PMID: 8041503
24. Shinohara K, Honma S, Katsuno Y, Abe H, Honma K. Two distinct oscillators in the rat suprachiasmatic nucleus in vitro. *Proc Natl Acad Sci U S A.* 1995; 92: 7396–400. Available: <http://www.ncbi.nlm.nih.gov/pubmed/7638204> <https://doi.org/10.1073/pnas.92.16.7396> PMID: 7638204
25. Noguchi T, Watanabe K, Ogura A, Yamaoka S. The clock in the dorsal suprachiasmatic nucleus runs faster than that in the ventral. *Eur J Neurosci.* 2004; 20: 3199–3202. <https://doi.org/10.1111/j.1460-9568.2004.03784.x> PMID: 15579176
26. Noguchi T, Watanabe K. Regional differences in circadian period within the suprachiasmatic nucleus. *Brain Res.* 2008; 1239: 119–126. <https://doi.org/10.1016/j.brainres.2008.08.082> PMID: 18801342

27. He PJ, Hirata M, Yamauchi N, Hashimoto S, Hattori MA. Gonadotropic regulation of circadian clockwork in rat granulosa cells. *Mol Cell Biochem.* 2007; 302: 111–118. <https://doi.org/10.1007/s11010-007-9432-7> PMID: 17483911
28. Inagaki N, Honma S, Ono D, Tanahashi Y, Honma KI. Separate oscillating cell groups in mouse suprachiasmatic nucleus couple photoperiodically to the onset and end of daily activity. *Proc Natl Acad Sci U S A.* 2007; 104: 7664–7669. <https://doi.org/10.1073/pnas.0607713104> PMID: 17463091
29. Nakamura W, Honma S, Shirakawa T, Honma KI. Clock mutation lengthens the circadian period without damping rhythms in individual SCN neurons. *Nat Neurosci.* 2002; 5: 399–400. <https://doi.org/10.1038/nn843> PMID: 11953751
30. Nagano M, Adachi A, Masumoto K, Hei, Meyer-Bernstein E, Shigeyoshi Y. rPer1 and rPer2 induction during phases of the circadian cycle critical for light resetting of the circadian clock. *Brain Res.* 2009; 1289: 37–48. <https://doi.org/10.1016/j.brainres.2009.06.051> PMID: 19559014
31. Natsubori A, Honma K, Ichi, Honma S. Differential responses of circadian Per2 rhythms in cultured slices of discrete brain areas from rats showing internal desynchronization by methamphetamine. *Eur J Neurosci.* 2013; 38: 2566–2571. <https://doi.org/10.1111/ejn.12265> PMID: 23725367
32. Yoshikawa T, Matsuno A, Yamanaka Y, Nishide S, ya, Honma S, Honma K, Ichi. Daily exposure to cold phase-shifts the circadian clock of neonatal rats in vivo. *Eur J Neurosci.* 2013; 37: 491–497. <https://doi.org/10.1111/ejn.12052> PMID: 23167790
33. Yamanaka Y, Honma S, Honma KI. Scheduled exposures to a novel environment with a running-wheel differentially accelerate re-entrainment of mice peripheral clocks to new light-dark cycles. *Genes to Cells.* 2008; 13: 497–507. <https://doi.org/10.1111/j.1365-2443.2008.01183.x> PMID: 18429821
34. Sujino M, Asakawa T, Nagano M, Koinuma S, Masumoto KH, Shigeyoshi Y. CLOCK $\Delta$ 19 mutation modifies the manner of synchrony among oscillation neurons in the suprachiasmatic nucleus. *Sci Rep.* 2018; 8: 1–14. <https://doi.org/10.1038/s41598-018-19224-1> PMID: 29339832
35. Ono D, Honma S, Honma K, Ichi. Differential roles of AVP and VIP signaling in the postnatal changes of neural networks for coherent circadian rhythms in the SCN. *Sci Adv.* 2016; 2: 1–12. <https://doi.org/10.1126/sciadv.1600960> PMID: 27626074
36. Nakamura W, Honma S, Shirakawa T, Honma KI. Regional pacemakers composed of multiple oscillator neurons in the rat suprachiasmatic nucleus. *Eur J Neurosci.* 2001; 14: 666–674. <https://doi.org/10.1046/j.0953-816x.2001.01684.x> PMID: 11556891
37. Mieda M, Ono D, Hasegawa E, Okamoto H, Honma K, Ichi, Honma S, et al. Cellular clocks in AVP neurons of the scn are critical for interneuronal coupling regulating circadian behavior rhythm. *Neuron.* 2015; 85: 1103–1116. <https://doi.org/10.1016/j.neuron.2015.02.005> PMID: 25741730
38. Hamnett R, Chesham JE, Maywood ES, Hastings MH. The Cell-Autonomous Clock of VIP Receptor VPAC2 Cells Regulates Period and Coherence of Circadian Behavior. *J Neurosci.* 2021; 41: 502–512. <https://doi.org/10.1523/JNEUROSCI.2015-20.2020> PMID: 33234609
39. Masumoto KH, Nagano M, Takashima N, Hayasaka N, Hiyama H, Matsumoto SI, et al. Distinct localization of prokineticin 2 and prokineticin receptor 2 mRNAs in the rat suprachiasmatic nucleus. *Eur J Neurosci.* 2006; 23: 2959–2970. <https://doi.org/10.1111/j.1460-9568.2006.04834.x> PMID: 16819985
40. Shan Y, Abel JH, Li Y, Izumo M, Cox KH, Jeong B, et al. Dual-Color Single-Cell Imaging of the Suprachiasmatic Nucleus Reveals a Circadian Role in Network Synchrony. *Neuron.* 2020; 108: 164–179.e7. <https://doi.org/10.1016/j.neuron.2020.07.012> PMID: 32768389
41. Pittendrigh CS, Daan S. A functional analysis of circadian pacemakers in nocturnal rodents—V. Pacemaker structure: A clock for all seasons. *J Comp Physiol A.* 1976; 106: 333–355. <https://doi.org/10.1007/BF01417860>
42. Yan L, Foley NC, Bobula JM, Kriegsfeld LJ, Silver R. Two antiphase oscillations occur in each suprachiasmatic nucleus of behaviorally split hamsters. *J Neurosci.* 2005; 25: 9017–26. <https://doi.org/10.1523/JNEUROSCI.2538-05.2005> PMID: 16192393
43. Daan S, Albrecht U, Van Der Horst GTJ, Illnerová H, Roenneberg T, Wehr TA, et al. Assembling a clock for all seasons: Are there M and E oscillators in the genes? *J Biol Rhythms.* 2001; 16: 105–116. <https://doi.org/10.1177/074873001129001809> PMID: 11302553
44. Jagota A, De La Iglesia HO, Schwartz WJ. Morning and evening circadian oscillations in the suprachiasmatic nucleus in vitro. *Nat Neurosci.* 2000; 3: 372–376. <https://doi.org/10.1038/73943> PMID: 10725927
45. Yoshikawa T, Inagaki NF, Takagi S, Kuroda S, Yamasaki M, Watanabe M, et al. Localization of photo-period responsive circadian oscillators in the mouse suprachiasmatic nucleus. *Sci Rep.* 2017; 7: 1–13. <https://doi.org/10.1038/s41598-017-08186-5> PMID: 28811515